0026-895X/06/6901-236–246$20.00
MOLECULAR PHARMACOLOGY
Copyright © 2006 The American Society for Pharmacology and Experimental Therapeutics
Mol Pharmacol 69:236–246, 2006

Vol. 69, No. 1
17814/3070298
Printed in U.S.A.

Probing the Molecular Mechanism of Interaction between 4-*n*-Butyl-1-[4-(2-methylphenyl)-4-oxo-1-butyl]-piperidine (AC-42) and the Muscarinic M_1 Receptor: Direct Pharmacological Evidence That AC-42 Is an Allosteric Agonist

Christopher J. Langmead, Victoria A. H. Fry, Ian T. Forbes, Clive L. Branch, Arthur Christopoulos, Martyn D. Wood, and Hugh J. Herdon

Psychiatry Centre of Excellence for Drug Discovery, GlaxoSmithKline, Harlow, Essex, United Kingdom (C.J.L., V.A.H.F., I.T.F., C.L.B., M.D.W., H.J.H.); and Department of Pharmacology, University of Melbourne, Parkville, Victoria, Australia (A.C.)

Received August 8, 2005; accepted October 5, 2005

ABSTRACT

4-*n*-Butyl-1-[4-(2-methylphenyl)-4-oxo-1-butyl]-piperidine hydrogen chloride (AC-42) is a selective agonist of the muscarinic M_1 receptor previously suggested to interact with an "ectopic" site on this receptor. However, the pharmacological properties of this site (i.e., whether it overlaps to any extent with the classic orthosteric site or represents a novel allosteric site) remain undetermined. In the present study, atropine or pirenzepine significantly inhibited the ability of either carbachol or AC-42 to stimulate inositol phosphate accumulation or intracellular calcium mobilization in Chinese hamster ovary (CHO) cells stably expressing the human M_1 receptor. However, the interaction between either of these antagonists and AC-42 was characterized by Schild slopes significantly less than unity. Increasing the concentrations of atropine revealed that the Schild regression was curvilinear, consistent with a negative allosteric interaction. More direct evidence for an allosteric mode of action of AC-42 was obtained in [^{3}H]*N*-methylscopolamine ([^{3}H]NMS) binding studies, in that both AC-42 and the prototypical modulator gallamine failed to fully inhibit specific [^{3}H]NMS binding in a manner that was quantitatively described by an allosteric model applied to both modulator data sets. Furthermore, AC-42 and gallamine significantly retarded the rate of [^{3}H]NMS dissociation from CHO-hM_1 cell membranes, conclusively demonstrating their ability to bind to a topographically distinct site to change M_1 receptor conformation. These data provide the first direct evidence that AC-42 is an allosteric agonist that activates M_1 receptors in the absence of the orthosteric agonist.

Muscarinic acetylcholine receptors (mAChRs) are members of the rhodopsin-like G protein-coupled receptor superfamily (Kristiansen, 2004). There are five known mAChR subtypes (M_1–M_5). M_1, M_3, and M_5 subtypes couple predominantly through the $G_{q/11}$ pathway to stimulate phospholipase C to catalyze the breakdown of phosphatidylinositol bisphosphate to inositol triphosphate and diacylglycerol and the subsequent mobilization of intracellular calcium (Caulfield and Birdsall, 1998). The M_2 and M_4 subtypes couple predominantly through the $G_{i/o}$ family of G proteins to inhibit adenylyl cyclase and decrease the intracellular level of cAMP (Caulfield and Birdsall, 1998).

There is a wide array of pharmacological tools with which to study mAChRs. *N*-Methyl scopolamine (NMS), quinuclidinyl benzilate, pirenzepine, and darifenacin, among mAChR antagonists, and acetylcholine and oxotremorine-M, among mAChR agonists, have been radiolabeled and used extensively to characterize mAChRs. Unfortunately, most of these pharmacological tools show low selectivity between mAChR subtypes (Caulfield and Birdsall, 1998; Ellis, 2002). This reflects the high level of conservation among the residues forming the orthosteric binding site of mAChRs, which makes the design of subtype-selective agonists and antagonists extremely difficult. An alternative route to engendering subtype selectivity among ligands targeted to the mAChRs is

A.C. is a Senior Research Fellow of the National Health and Medical Research Council of Australia. Article, publication date, and citation information can be found at http://molpharm.aspetjournals.org.
doi:10.1124/mol.105.017814.

ABBREVIATIONS: mAChR, muscarinic acetylcholine receptor; NMS, *N*-methyl scopolamine; C_7/3-phth, heptane-1,7-bis-(dimethyl-3′-phthalimidopropyl)-ammonium bromide; TM, transmembrane; AC-42, 4-*n*-butyl-1-[4-(2-methylphenyl)-4-oxo-1-butyl]-piperidine; IP, inositol phosphate; CHO, Chinese hamster ovary; FLIPR, fluorometric imaging plate reader; IF, inositol-free; DMEM, Dulbecco's modified Eagle's medium; PD 81,723, (2-amino-4,5-dimethyl-3-thienyl)(3-(trifluoromethyl)phenyl)-methanone; McN-A-343, 4-(*m*-chlorophenyl-carbamoyloxy)-2-butynyltrimethylammonium chloride.

through search for allosteric modulators, which act at a site that is topographically distinct from the orthosteric binding site.

Allosteric modulators of mAChRs represent some of the best-characterized examples of allosterism at G protein-coupled receptors. Ligands such as gallamine, alcuronium, heptane-1,7-bis-(dimethyl-3′-phthalimidopropyl)-ammonium bromide (C_7/3-phth), brucine, and closely related analogs have all been shown to have varying allosteric effects on mAChRs depending on the interacting orthosteric ligand. The ability of the same allosteric modulator to display different types of cooperative interactions (positive, negative, or neutral) depending on the nature of the ligand occupying the orthosteric site is characteristic of allosteric interactions, a phenomenon previously referred to as "probe dependence" (Christopoulos and Kenakin, 2002).

The best-studied examples of mAChR allosteric modulators, as described above, are thought to interact at a site near, but extracellular to, the orthosteric binding site (Gnagey et al., 1999). Site-directed mutagenesis studies suggest that the interaction with residues at the top of TM7 and in extracellular loops 2 and 3 is responsible for the different mAChR selectivities exhibited by these ligands (Matsui et al., 1995; Gnagey et al., 1999). Spalding et al. (2002) have described a novel compound, AC-42 (Fig. 1), which activated the M_1 receptor with an intrinsic activity of approximately 0.7 compared with the traditional orthosteric agonist carbachol but had no significant agonist activity at the M_2–M_5 mAChRs despite binding to all subtypes with similar affinity (Spalding et al., 2002). Chimeric receptor studies indicated that the N terminus-TM1 and extracellular loop 3-TM7 regions of the M_1 mAChR were required to play a role in the selective activation of the receptor by AC-42 (Spalding et al., 2002); regions that are not consistent with AC-42 binding to the orthosteric site of the M_1 mAChR deeper in the TM bundle. In an elegant conclusion to their study, Spalding et al. (2002) demonstrated that the potency of AC-42 was not significantly attenuated by either of the point mutations Y381A or N382A in TM6; residues that are believed to form part of the orthosteric site in that their mutation abolishes the agonist activity of carbachol (Ward et al., 1999; Spalding et al., 2002). These findings prompted the authors to categorize AC-42 as an "ectopic" agonist, in the knowledge that its binding site is partially or totally distinct from that for carbachol, but in the absence of definitive pharmacological data proving that it is an allosteric ligand.

To date, the molecular relationship among the binding site used by AC-42, the orthosteric site used by traditional mAChR ligands, and the allosteric site used by prototypical allosteric modulators remains undetermined. If the ectopic site is actually a completely distinct allosteric site, then this would have profound implications for drug discovery, because it would represent the most striking example of a selective allosteric agonist identified to date for any G protein-coupled receptor. In this study, we have used a combination of functional calcium mobilization, inositol phosphate (IP) accumulation, and radioligand inhibition and dissociation kinetic binding assays to characterize the molecular nature of the interaction between AC-42 and the M_1 mAChR. We provide, for the first time, direct evidence that AC-42 is an allosteric agonist of this receptor.

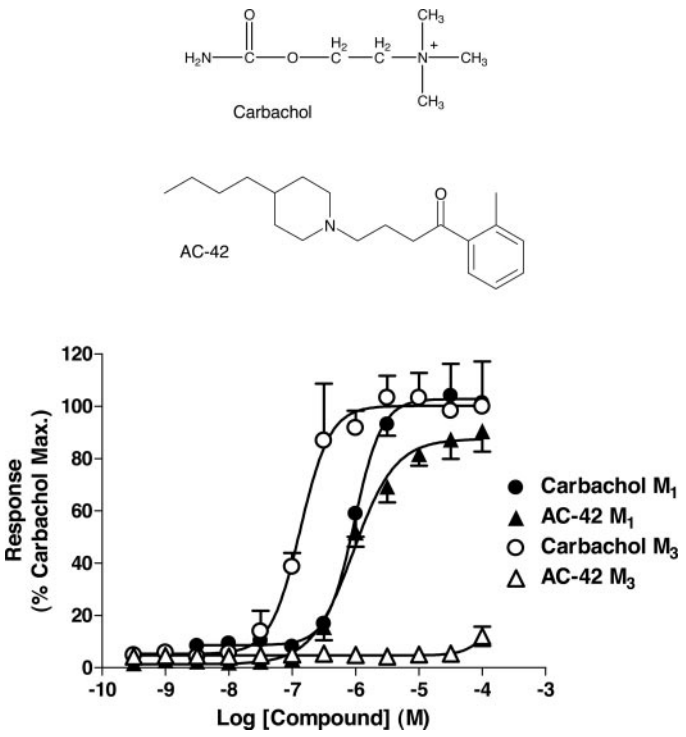

Fig. 1. Concentration-dependent stimulation of IP accumulation in CHO-hM_1 and CHO-hM_3 cells by carbachol and AC-42. Data are the mean of at least three independent experiments (±S.E.M.). Also shown are the structures of carbachol and AC-42.

Materials and Methods

Materials. All cell culture reagents were from Invitrogen (Paisley, UK). *myo*-[^{3}H]Inositol and [^{3}H]NMS were from GE Healthcare (Little Chalfont, Buckinghamshire, UK). AC-42 was synthesized in house. All other chemicals were purchased from Sigma Chemical (Poole, Dorset, UK) or BDH (Poole, Dorset, UK).

Cell Culture. CHO-hM_1 and CHO-hM_3 cells were routinely cultured in α-minimal essential medium with ribonucleosides plus 10% fetal bovine serum. Cells were kept in a humidified atmosphere at 37°C in 5% CO_2 and passaged twice weekly by scraping in media, centrifugation (200*g*; 5 min), and resuspension of the pellet in fresh media.

CHO-hM_1 Calcium Mobilization Assays. Intracellular calcium was monitored using the fluorescent wash-free dye Calcium Plus (Molecular Devices, Reading, UK) in a fluorometric imaging plate reader (FLIPR; Molecular Devices). CHO-hM_1 cells were seeded into clear-bottomed black-walled 96-well microtiter plates (Costar UK Ltd., High Wycombe, Buckinghamshire, UK) 24 h before use at a density of 50,000 cells/well. Before assay on a FLIPR, medium was removed, and cells were incubated with Calcium Plus according to manufacturer's instructions for 60 min at 37°C in Tyrode's buffer (145 mM NaCl, 2.5 mM KCl, 1.2 mM $MgCl_2$, 10 mM Na-HEPES, 10 mM glucose, and 1.5 mM $CaCl_2$, pH 7.4) containing 2.5 mM probenecid. For agonist studies, compounds were tested for activity in a FLIPR assay by adding 50 μl of test solution into a plate volume of 50 μl. For antagonist studies, cells were preincubated with antagonist or buffer, for 30 min before agonist addition on the FLIPR (50 μl of test solution into a plate volume of 100 μl). Fluorescence was monitored (λ_{ex} = 488 nm, λ_{EM} = 540 nm) before and after the addition of agonist at 1-s intervals for 60 s and at 5 s intervals for a further 60 s. Agonist concentration-response curves were constructed using the peak stimulation (minus basal) for each concentration of agonist.

Inositol Phosphate Accumulation Scintillation Proximity Assay. Inositol phosphate accumulation scintillation proximity assays were carried out as described in Brandish et al. (2003) with minor modifications. CHO-hM_1 or CHO-hM_3 cells were seeded into clear-bottomed black-walled 96-well microtiter plates (Costar UK Ltd.) at a density of 50,000 cells/well. After 24 h, the cell medium was removed and replaced with 100 μl of inositol-free (IF) DMEM containing 10 μCi/ml *myo*-[^{3}H]inositol (GE Healthcare). After 16 h, the *myo*-[^{3}H]inositol was removed, and the cells washed with 2 $\times$ 200 μl of IF-DMEM. Cells were then incubated with 100 μl of agonist and 100 μl of antagonist/media in IF-DMEM containing 5 mM LiCl for 1 h at 37°C. The reaction was terminated by the removal of the medium and the addition of 200 μl of 0.1 M formic acid (Sigma Chemical) to extract inositol phosphates. The extraction was allowed to continue for 1 h at room temperature after which 20-μl samples of the extracts were removed from each well and combined with 80 μl of RNA binding yttrium silicate scintillation proximity assay beads (12.5 mg/ml) in opaque-bottomed 96-well picoplates (PerkinElmer Life and Analytical Sciences, Boston, MA). Plates were agitated for 1 h at room temperature, and then the beads were left to settle for 2 h. Total [^{3}H]inositol phosphate accumulation (cpm) for each concentration of agonist was determined on a TopCount plate counter (PerkinElmer Life and Analytical Sciences) and used to construct concentration-response curves.

CHO-hM_1 Cell Membrane Preparation. Cell membrane preparation was carried out as described in Lanzafame and Christopoulos (2004); all procedures were carried out at 4°C. CHO-hM_1 cells were harvested as described above. The cell pellet was resuspended in 5 ml of ice-cold buffer containing 50 mM Tris-HCl, 3 mM $MgCl_2$, and 0.2 mM EGTA, pH 7.4, and then homogenized using an Ultra-Turrax homogenizer (IKA-Werke GmbH, Staufen, Germany) for 30 s. The homogenate was centrifuged at 1000*g* for 10 min, the remaining pellet was discarded, and the supernatant re-centrifuged at 39,000*g* for 30 min. The resulting cell membrane pellet was resuspended in the same buffer at a protein concentration of 2 mg/ml as determined by the method of Bradford (1976). Aliquots were stored at −80°C until further use.

CHO-hM_1 [^{3}H]NMS Inhibition Binding Assays. Inhibition binding studies were performed by incubating CHO-hM_1 cell membranes (10 μg of protein/well) with [^{3}H]NMS (0.2 or 2 nM) and a range of concentrations of the test compound at 37°C for 1 h in buffer containing 50 mM HEPES, 110 mM NaCl, 5.4 mM KCl, 1.8 mM $CaCl_2$, 1 mM $MgSO_4$, 25 mM glucose, and 58 mM sucrose, pH 7.4. The final assay volume was 0.5 ml. Compounds were serially diluted in HEPES buffer to generate 10 different test concentrations over a 5 log unit range. Nonspecific binding was defined as that remaining in the presence of 1 μM atropine. The reaction was terminated by rapid filtration through GF/B filter mates presoaked in double distilled H_2O using a 48-well Brandel cell harvester (Semat International, Ltd., St. Albans, Herts, UK) Filters were washed with 5 $\times$ 1 ml of ice-cold 0.9% (w/v) NaCl solution and allowed to dry before bound radioactivity was measured using liquid scintillation counting.

CHO-hM_1 [^{3}H]NMS Kinetic Binding Assays. For dissociation studies, CHO-hM_1 cell membranes (10 μg of protein/well) were preincubated with [^{3}H]NMS (0.2 nM) and either HEPES buffer or atropine (1 μM final) for 60 min in a final assay volume of 0.55 ml. Triplicate determinations of total and nonspecific binding of [^{3}H]NMS, as defined above, were then measured at 0.5, 1, 2, 5, 10, 20, and 30 min after the addition of atropine (1 μM final) either in the presence or absence of AC-42 (100 μM final) or gallamine (1 mM final). Buffer composition, reaction termination, and radioactivity determination were all as for CHO-hM_1 inhibition binding.

Data Analysis. For the functional assays, agonist concentration-response curves, in the absence and presence of antagonist, were globally fitted to the following logistic equation (Motulsky and Christopoulos, 2004) using Prism 4 (GraphPad Software Inc., San Diego, CA):

$$Y = Bottom + \frac{(Top - Bottom)}{1 + \left(\frac{10^{\log EC_{50}}[1 + ([B]/10^{-pA_2})^s]}{[A]}\right)^{n_H}} \quad (1)$$

where *Top* represents the maximal asymptote of the curves, *Bottom* represents the lowest asymptote (basal response) of the curves, log EC_{50} represents the logarithm of the agonist EC_{50} in the absence of antagonist, [A] represents the concentration of the agonist, [B] represents the concentration of the antagonist, n_H represents the Hill slope of the agonist curve, s represents the Schild slope for the antagonist, and pA_2 represents the negative logarithm of the concentration of antagonist that shifts the agonist EC_{50} by a factor of 2. In the absence of antagonist ([B] = 0), this equation becomes the standard four-parameter logistic equation for fitting agonist concentration-response data. When fitting agonist concentration-response data obtained in the presence of antagonist, if the estimated Schild slope was not significantly different from unity, it was constrained as such and the estimate of pA_2 represented the pK_B. For presentation purposes, concentration-ratios were also derived for the concentration-response curves in the absence or presence of antagonist and plotted in the form of a Schild regression (Kenakin, 1997). Where appropriate, concentration-response data were also fitted to the following equation, which is based on a simple allosteric ternary complex model of ligand-receptor interaction (Ehlert, 1988; Lazareno and Birdsall, 1995; Christopoulos and Kenakin, 2002):

$$Y = Bottom + \frac{(Top - Bottom)}{1 + \left(\frac{10^{\log EC_{50}}\left(\frac{1 + [B]/K_B}{1 + \alpha\,[B]/K_B}\right)}{[A]}\right)^{n_H}} \quad (2)$$

where *Top*, *Bottom*, log EC_{50}, n_H, and [A] are as described above for eq. 1, [B] denotes the concentration of allosteric ligand, K_B denotes its equilibrium dissociation constant for binding to the allosteric site on the receptor, and α denotes the cooperativity factor, which is a thermodynamic measure of the strength of allosteric interaction between the orthosteric and allosteric sites. Values of $\alpha > 1$ denote positive cooperativity (allosteric enhancement), whereas values of $\alpha < 1$ denote negative cooperativity (allosteric inhibition).

Radioligand inhibition binding isotherms for the interaction between two different concentrations of [^{3}H]NMS and either atropine or pirenzepine were globally fitted according to the following one-site orthosteric mass-action equation:

$$Y = Bottom + \frac{(Top - Bottom)}{1 + \frac{[B]}{K_B\left(1 + \frac{[A]}{K_A}\right)}} \quad (3)$$

where Y denotes the percentage of specific binding; *Top* and *Bottom* denote the maximal and minimal asymptotes, respectively; [A] denotes the concentration of [^{3}H]NMS (either 0.2 or 2 nM); [B] denotes the unlabeled antagonist concentration; and K_A and K_B denote the equilibrium dissociation constants of A and B, respectively. For each series of antagonist curves, the negative logarithm of the K_A value for [^{3}H]NMS was fixed at 9.6 (determined separately in saturation binding assays), and the K_B parameter was constrained to be shared across both curves.

Radioligand inhibition binding isotherms for the interaction between two different concentrations of [^{3}H]NMS and either AC-42 or gallamine were globally fitted according to the following equation, based on the simple ternary complex model of allosteric interaction:

$$\frac{Y}{Y_{max}} = \frac{[A]}{[A] + \frac{K_A(1 + [B]/K_B)}{(1 + \alpha[B]/K_B)}} \quad (4)$$

where Y/Y_{max} denotes fractional receptor occupancy, [A] and K_A are as defined for eq. 3 above, and [B], K_B, and α are as described for eq. 2 above. For each series of inhibition curves, the negative logarithm of the K_A value for [^{3}H]NMS was fixed at 9.6 (as above), and the K_B and α parameters were constrained to be shared across both curves.

For the dissociation kinetic experiments, dissociation curves for the radioligand, in the absence and presence of applied modulator, were evaluated by nonlinear regression using the following equation:

$$B_t = B_0 \cdot e^{-k_{offobs} \cdot t} \quad (5)$$

where B_t denotes the specific binding of radioligand at time t, B_0 denotes the specific binding of radioligand at equilibrium (time = 0), and k_{offobs} denotes the observed radioligand dissociation rate constant. For the gallamine/[^{3}H]NMS dissociation kinetic experiments, data sets were globally fitted to eq. 5 with the parameter k_{offobs} defined as follows.

$$k_{offobs} = \frac{[B] \cdot \frac{k_{offB}}{K_B/\alpha} + k_{off}}{1 + \frac{[B]}{K_B/\alpha}} \quad (6)$$

where k_{off} denotes the rate constant for dissociation of the radioligand from the free (unoccupied) receptor, k_{offB} denotes the rate constant for the dissociation of the radioligand from the modulator-occupied receptor (fixed to zero for this analysis; see *Results*), and K_B/α denotes the dissociation constant of the modulator for the radioligand-occupied receptor (Lazareno and Birdsall, 1995; Christopoulos et al., 1999). Note that in the absence of modulator, $k_{offobs} = k_{off}$.

In all cases, potency, affinity, and cooperativity values were estimated as logarithms (Christopoulos, 1998). Data shown are the mean ± S.E.M. Comparisons between mean values were performed by F-test. Unless otherwise stated, values of $p < 0.05$ were taken as statistically significant.

Results

Functional Analyses of Agonist-Antagonist Interactions. Both carbachol and AC-42 stimulated IP accumulation in CHO-hM_1 cells, with pEC_{50} values of 6.35 ± 0.02 and 6.21 ± 0.10, respectively (Fig. 1). AC-42 was a partial agonist with respect to carbachol (F-test; $p < 0.001$), with an intrinsic activity of 0.85. Although carbachol also caused a robust stimulation of IP accumulation in CHO-hM_3 cells (pEC_{50} = 6.81 ± 0.04), AC-42 did not show any appreciable agonist activity at this mAChR subtype at concentrations up to 100 μM (Fig. 1).

Subsequent IP accumulation assays investigated the interaction between carbachol or AC-42 and the nonselective mAChR antagonist atropine or the relatively M_1-selective antagonist pirenzepine. As shown in Fig. 2, both atropine and pirenzepine produced concentration-dependent rightward shifts in the concentration-response curve to carbachol, with no significant effect on the basal or maximal agonist response, and with Schild slopes not significantly different from unity (Table 1). Because this behavior is consistent with the expectations of simple orthosteric antagonism (Kenakin, 1997), pK_B values for each antagonist were also calculated and are shown in Table 1. It is noteworthy that when these experiments were repeated with AC-42 rather than carbachol as the agonist, a different pattern of behavior was noted. In particular, although both atropine and pirenzepine produced concentration-dependent rightward shifts in the concentration-response curve to AC-42 with no significant effect on the basal or maximal agonist response (Fig. 3), the magnitude of these shifts deviated significantly from that expected for orthosteric antagonism. This was manifested as a Schild slope significantly less than 1 for each antagonist (Table 2) and because the AC-42/antagonist IP data did not satisfy the minimum criteria expected for orthosteric antagonism, a pK_B value was not determined. However, a pA_2 value was still calculated, using eq. 1 under *Materials and Methods*, as an empirical measure of antagonist potency (Table 2).

To complement the IP accumulations assays, additional experiments were performed using intracellular calcium mobilization as the functional readout. Both carbachol and AC-42 stimulated calcium mobilization in CHO-hM_1 cells with pEC_{50} values of 8.38 ± 0.11 and 7.15 ± 0.12, respectively. Moreover, both ligands were now full agonists in this assay.

Figure 4 illustrates the interaction between carbachol or AC-42 with pirenzepine in the calcium mobilization assay. In agreement with the results of the IP accumulation assay, the interaction between carbachol and pirenzepine (Fig. 4A) was completely consistent with simple orthosteric antagonism; the resulting Schild slope and pK_B values are shown in Table 1, where it can also be seen that there was no significant difference between the pK_B estimates for pirenzepine from either assay. In contrast, but in agreement with the findings from the IP accumulation assays, the interaction between AC-42 and pirenzepine was characterized by a Schild slope that was significantly less than 1 (Table 2). The estimated pA_2 value for this interaction is also shown in Table 2.

At the molecular level, Schild slopes that deviate significantly from unity may be indicative of a negative allosteric interaction between agonist and antagonist (Christopoulos and Kenakin, 2002). In this instance, the reduction in Schild slope reflects the saturability of the negative allosteric interaction, because increasing the concentration of one ligand results in a progressive inability to further antagonize the other ligand. To experimentally confirm that this was the case, a large range of antagonist concentrations was tested in an attempt to reveal saturable antagonism (Christopoulos and Kenakin, 2002). Figure 5 shows the results of calcium mobilization experiments that were specifically designed to investigate whether the interaction between atropine and AC-42 was mechanistically and quantitatively consistent with an allosteric model of interaction. When tested against the classic orthosteric agonist carbachol, atropine inhibited M_1 receptor-mediated calcium mobilization in a manner completely consistent with orthosteric antagonism; i.e., the Schild slope was not significantly different from unity over concentrations of antagonist spanning 6 orders of magnitude (Fig. 5A). In contrast, the ability of the highest concentrations of atropine to inhibit the effects of AC-42 clearly approached a limiting value as exemplified by a curvilinear Schild regression (Fig. 5B). Analysis of the data set according to an orthosteric model (eq. 1 under *Materials and Methods*) yielded a Schild regression with a slope factor of 0.69 ± 0.01, significantly less than unity (Fig. 5B; Table 2). Because the AC-42/atropine data shown in Fig. 5 were consistent with a negative allosteric interaction, the data were fitted to the allosteric ternary complex model (eq. 2 under *Materials and Methods*), which yielded the parameter values listed in Table 2. From this analysis, the interaction between atropine and

AC-42 was characterized by an α value of ca. 0.0002. Statistical comparison of the fit according to the allosteric ternary complex model [eq. 2 and the fit according to eq. 1 in which the slope value was constrained to 1 (indicative of a true competitive interaction)] revealed a clear preference for the former (F-test; $p < 0.0001$).

[^{3}H]NMS Inhibition Binding Studies. The analysis of the functional data presented above assumes that the molecular mechanism governing the interaction between AC-42 and orthosteric antagonists, such as atropine, is an allosteric modification of ligand binding affinity (quantified by α). To probe and validate this proposed mechanism, radioligand binding assays were performed using [^{3}H]NMS as an orthosteric-site "probe". Both atropine and pirenzepine fully inhibited specific [^{3}H]NMS binding in membranes from CHO-hM_1 cells at radioligand concentrations of either 0.2 nM (ca. K_A) or 2 nM (ca. 10× K_A; Fig. 6A), as expected for simple orthosteric antagonism. A global analysis of each data set, according to eq. 3 under *Materials and Methods*, yielded pK_B values of 9.37 ± 0.04 for atropine and 7.99 ± 0.05 for pirenzepine. These values were also in excellent agreement with the pK_B values determined from the functional assays for these antagonists (Table 1).

Although AC-42 also inhibited [^{3}H]NMS binding in a concentration-dependent manner, it was unable to fully reduce specific binding levels to zero; this was more marked when the concentration of radioligand was increased 10-fold (Fig. 6B); an effect consistent with a saturability of antagonism characteristic of a negatively cooperative allosteric interaction. A global analysis of each pair of inhibition curves, according to the allosteric ternary complex model of interaction (eq. 4), yielded a pK_B value of 6.19 ± 0.07 as a measure of the

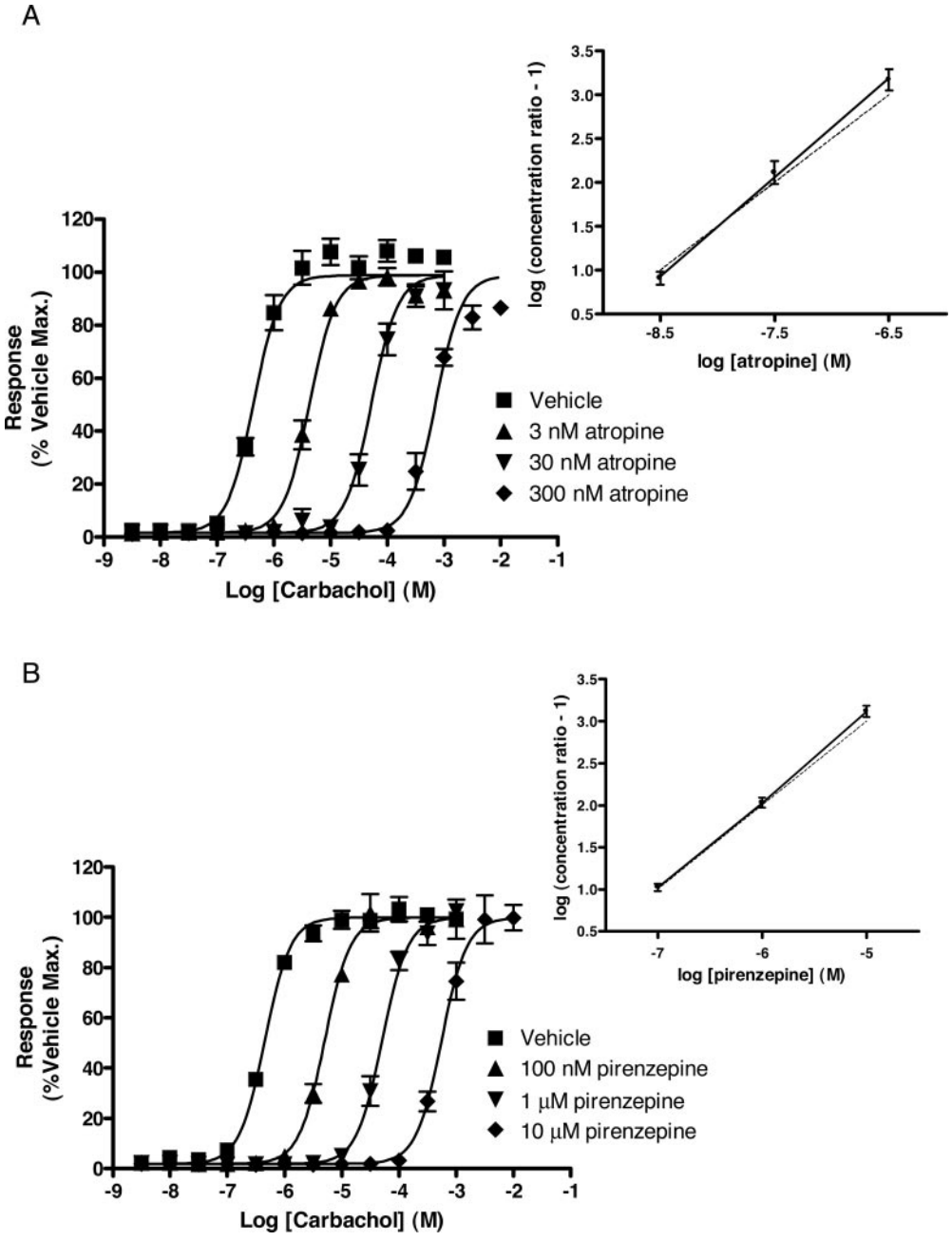

Fig. 2. Concentration-dependent antagonism of carbachol-stimulated IP accumulation in CHO-hM_1 cells by atropine (3 nM–300 nM) (A) and pirenzepine (100 nM–10 μM) (B) with inset Schild regressions. Dotted lines on Schild plots indicate a theoretical slope of 1. Data are the mean of at least three independent experiments (±S.E.M.).

affinity of AC-42 for its allosteric site on the unoccupied M_1 receptor, and a log α value of -1.66 ± 0.12 (i.e., $\alpha = 0.022$). The large difference between the cooperativity between AC-42 and atropine (0.0002) and that between AC-42 and [^{3}H]NMS is a striking example of the probe dependence of allosteric interactions.

For comparison, similar experiments were also performed with the well characterized and prototypical negative mAChR allosteric modulator gallamine. As expected, gallamine also displayed an inability to fully inhibit the specific binding of the radioligand (Fig. 6B). Global analysis of the two curves yielded estimates of $pK_B = 5.19 \pm 0.06$ and log $\alpha = -1.28 \pm 0.06$ ($\alpha = 0.053$).

[^{3}H]NMS Dissociation Binding Studies. Because allosteric modulators of G protein-coupled receptors cause a conformational change in the receptor that is often manifested as an alteration of the dissociation characteristics of a preformed orthosteric ligand-receptor complex (Kostenis and Mohr, 1996), [^{3}H]NMS dissociation kinetic assays were performed. Radioligand dissociation from CHO-hM_1 cell membranes under control conditions was rapid and monophasic, with a k_{off} value of 0.19 ± 0.02/min. The presence of gallamine (1 mM) produced a marked retardation of [^{3}H]NMS dissociation, yielding a k_{offobs} of 0.017 ± 0.001/min (Fig. 7; *t* test; $p < 0.01$). Because previous studies have shown that gallamine is able to completely prevent [^{3}H]NMS dissociation from mAChRs (Lazareno and Birdsall, 1995), the data were refitted to eq. 6, with the parameter, k_{offB}, constrained to a value of zero, yielding an estimate of the apparent affinity of gallamine for the [^{3}H]NMS-occupied receptor (log K_B/α) of -3.86 ± 0.12. This estimate is in excellent agreement with the expected value calculated using the pK_B and log α estimates derived from the inhibition binding assays (log $K_B/\alpha = -3.91$), further validating the allosteric ternary complex model as an appropriate mechanistic descriptor of the interactions measured in the current study.

It is noteworthy that AC-42 (100 μM) also significantly slowed the rate of [^{3}H]NMS dissociation, yielding a k_{offobs} value of 0.122 ± 0.005/min (Fig. 7; $p < 0.05$), although this effect was much less marked than that for gallamine. Because of the modest effect of AC-42 at a concentration that is close to its solubility limits, however, it was not possible to determine the maximum extent of its ability to retard [^{3}H]NMS dissociation. Nonetheless, the ability of AC-42 to significantly alter the dissociation rate of [^{3}H]NMS confirmed that this agonist is also an allosteric modulator.

TABLE 1

Parameters describing the functional interaction between the orthosteric antagonists atropine or pirenzepine and the agonist carbachol at M_1 mAChRs expressed in CHO cells

Values are the mean ± S.E.M. of three to four independent experiments. pK_B is the negative logarithm of the antagonist dissociation constant. pK_B and Schild slope are estimated by nonlinear regression according to eq. 1 under *Materials and Methods*.

Parameter	Orthosteric Antagonist	
	Atropine	Pirenzepine
IP accumulation		
pK_B	9.61 ± 0.05	8.05 ± 0.02
Schild slope	1.13 ± 0.05	1.04 ± 0.01
Calcium mobilization		
pK_B	9.66 ± 0.06	8.13 ± 0.04
Schild slope	1.00 ± 0.01	0.94 ± 0.03

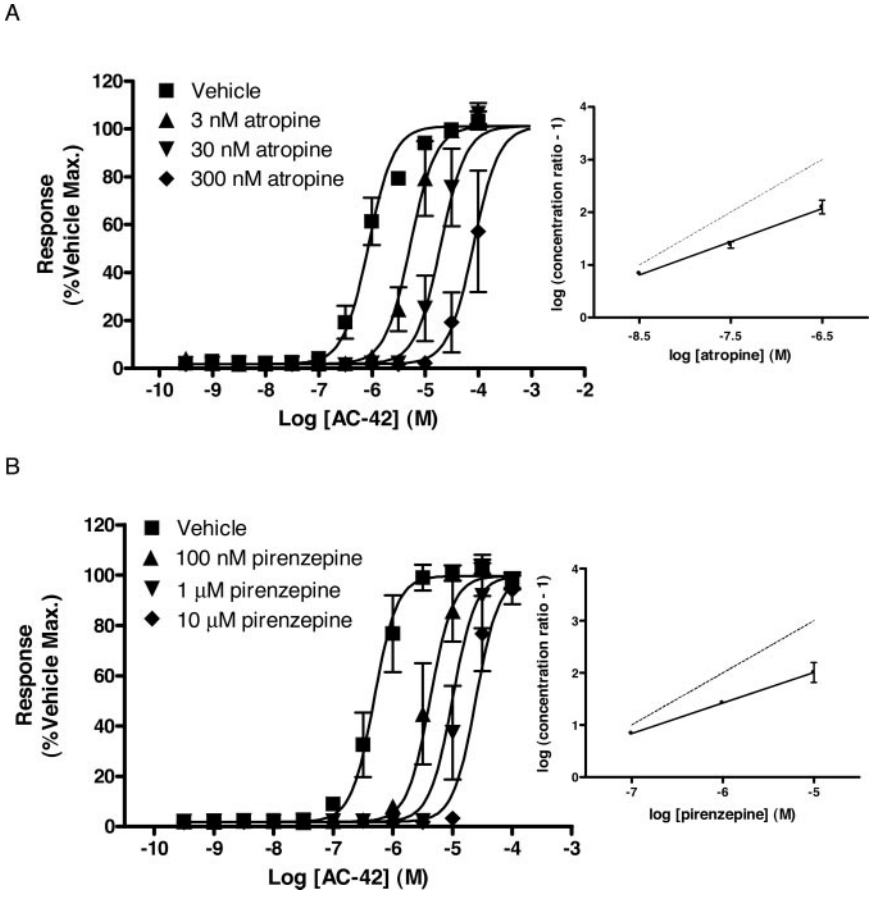

Fig. 3. Concentration-dependent antagonism of AC-42-stimulated IP accumulation in CHO-hM_1 cells by atropine (3 nM–300 nM) (A) and pirenzepine (100 nM-10 μM) (B) with inset Schild regressions. Dotted lines on Schild plots indicate a theoretical slope of 1. Data are the mean of at least three independent experiments (±S.E.M.).

Discussion

Our findings provide direct evidence that the functionally selective M_1 mAChR agonist AC-42 is an allosteric modulator. An investigation of the mode of interaction of this agonist with various orthosteric ligands confirmed that AC-42 exhibited characteristics associated with allosteric ligands, including 1) a saturability to its allosteric effects, 2) a dependence of these effects on the nature of the orthosteric ligand with which it interacted, and 3) the ability to significantly retard the dissociation of [^{3}H]NMS from the M_1 mAChR. These results reveal that the M_1 mAChR possesses an allosteric site capable of mediating receptor activation in its own right and further reinforce the utility of allosteric binding sites for achieving selectivity at G protein-coupled receptors.

In agreement with previous studies (Spalding et al., 2002; Sur et al., 2003), AC-42 caused a robust stimulation in both IP accumulation and intracellular calcium mobilization in CHO-hM_1 cells. The significantly higher potency for both agonists in the calcium assay, relative the IP assay, and the accompanying increase in maximal AC-42 response to match that of carbachol, are consistent with an increase in stimulus-response coupling resulting from signal amplification in the calcium response, which is downstream of the IP pathway. The partial agonist activity of AC-42 in the IP accumulation assay relative to carbachol is also consistent with the study by Spalding et al. (2002). Because partial agonists require maximal receptor occupancy to generate their maximal responses, the pEC_{50} value of a partial agonist is a useful approximation of its affinity for the receptor (Kenakin, 1997). It is thus noteworthy that the pEC_{50} in the IP accumulation assay (6.21) is in excellent agreement with the pK_B value

TABLE 2

Parameters describing the interaction between the orthosteric antagonists atropine or pirenzepine and the agonist AC-42 at M_1 mAChRs expressed in CHO cells

Values are the mean ± S.E.M. of three to four independent experiments. pA_2 is the empirical estimate of antagonist potency. pA_2 and Schild slope are estimated by nonlinear regression according to eq. 1 under *Materials and Methods*. pK_B is the negative logarithm of the antagonist dissociation constant and log α is the logarithm of the cooperativity factor, both estimated by nonlinear regression according to an allosteric ternary complex model (eq. 2 under *Materials and Methods*).

Parameter	Orthosteric Antagonist	
	Atropine	Pirenzepine
IP accumulation		
pA_2	9.65 ± 0.10	9.18 ± 0.04
Schild slope	0.63 ± 0.02***	0.41 ± 0.02***
Calcium mobilization		
Orthosteric fit		
pA_2	9.67 ± 0.10	8.16 ± 0.22
Schild slope	0.69 ± 0.01***	0.74 ± 0.06***
Allosteric fit		
pK_B	9.06 ± 0.06	N.D.
log α	−3.79 ± 0.07	N.D.

N.D., not determined.
*** Significantly different from unity ($p < 0.001$; F-test).

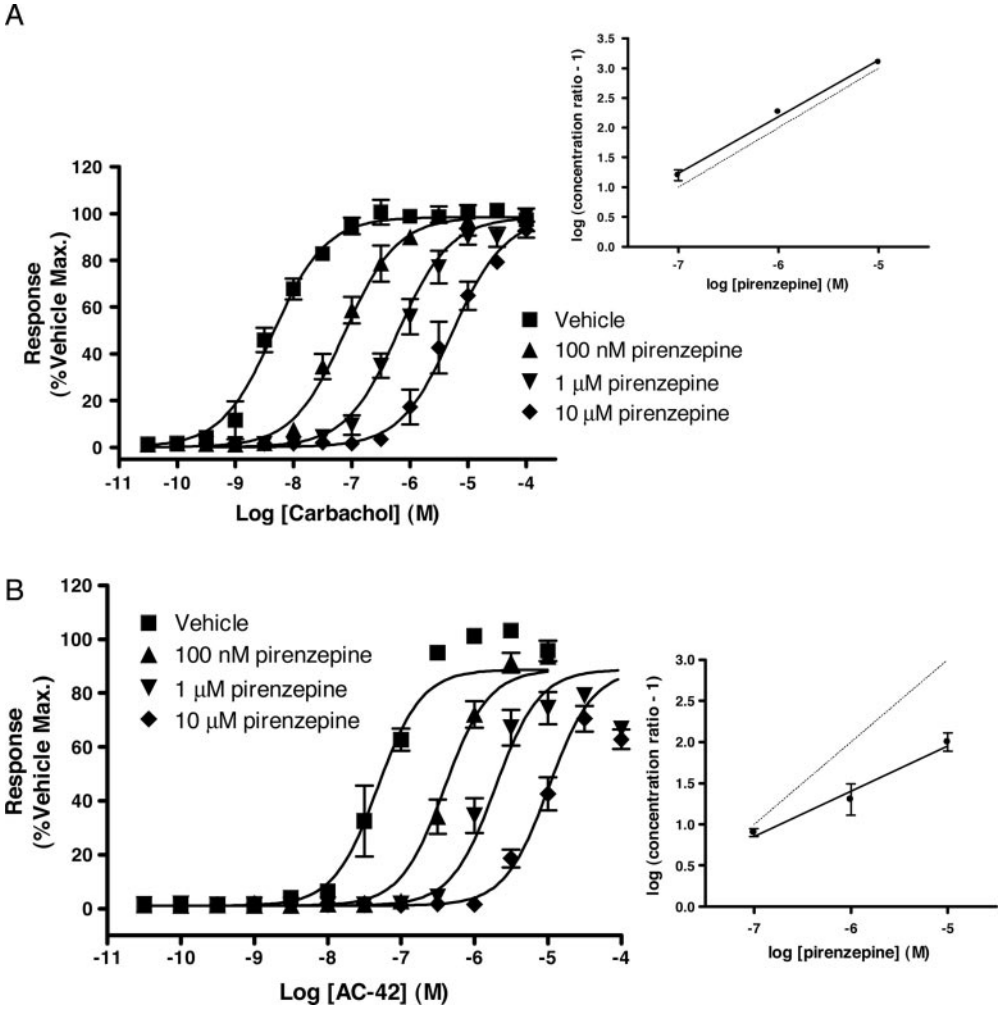

Fig. 4. Concentration-dependent antagonism of carbachol-stimulated (A) or AC-42-stimulated (B) calcium mobilization in CHO-hM_1 cells by pirenzepine (100 nM–10 μM) with inset Schild regressions. Dotted lines on Schild plots indicate a theoretical slope of 1. Data are the mean of at least three independent experiments (±S.E.M.).

estimated for the binding of AC-42 according to an allosteric model (6.19).

In functional assays, the best-characterized methods for investigating the mechanism of interaction between agonists and antagonists are the procedures underlying Schild analysis and its variants (Arunlakshana and Schild, 1959; Kenakin, 1997; Motulsky and Christopoulos, 2004). Atropine or pirenzepine antagonized the effects of carbachol in a manner that was consistent with competition for a common (orthosteric) binding site. This was most evident with atropine in the calcium mobilization assay, where a Schild slope of 1 was maintained over antagonist concentrations spanning 6 orders of magnitude (Fig. 5A). The resulting pK_B values (Table 1) were consistent with previously reported values in the literature for the binding of atropine or pirenzepine to the M_1 mAChR (Ellis, 2002). In contrast, the translocation of the AC-42 concentration-response curve by atropine or pirenzepine in either functional assay format led to Schild slopes significantly less than unity (Table 2), indicating that the antagonism was not consistent with a simple orthosteric interaction.

A clue to the underlying mechanism of action of AC-42 was provided by the atropine antagonism data in the calcium mobilization assay. Negative allosteric interactions have previously been demonstrated in functional assays by a progressive inability of the antagonist to shift the agonist concentration-response curve with increasing antagonist concentrations (Clark and Mitchelson, 1976; Lanzafame et al., 1996), yielding a characteristic curvilinear Schild regression. As shown in Fig. 5B, this was exactly the type of behavior

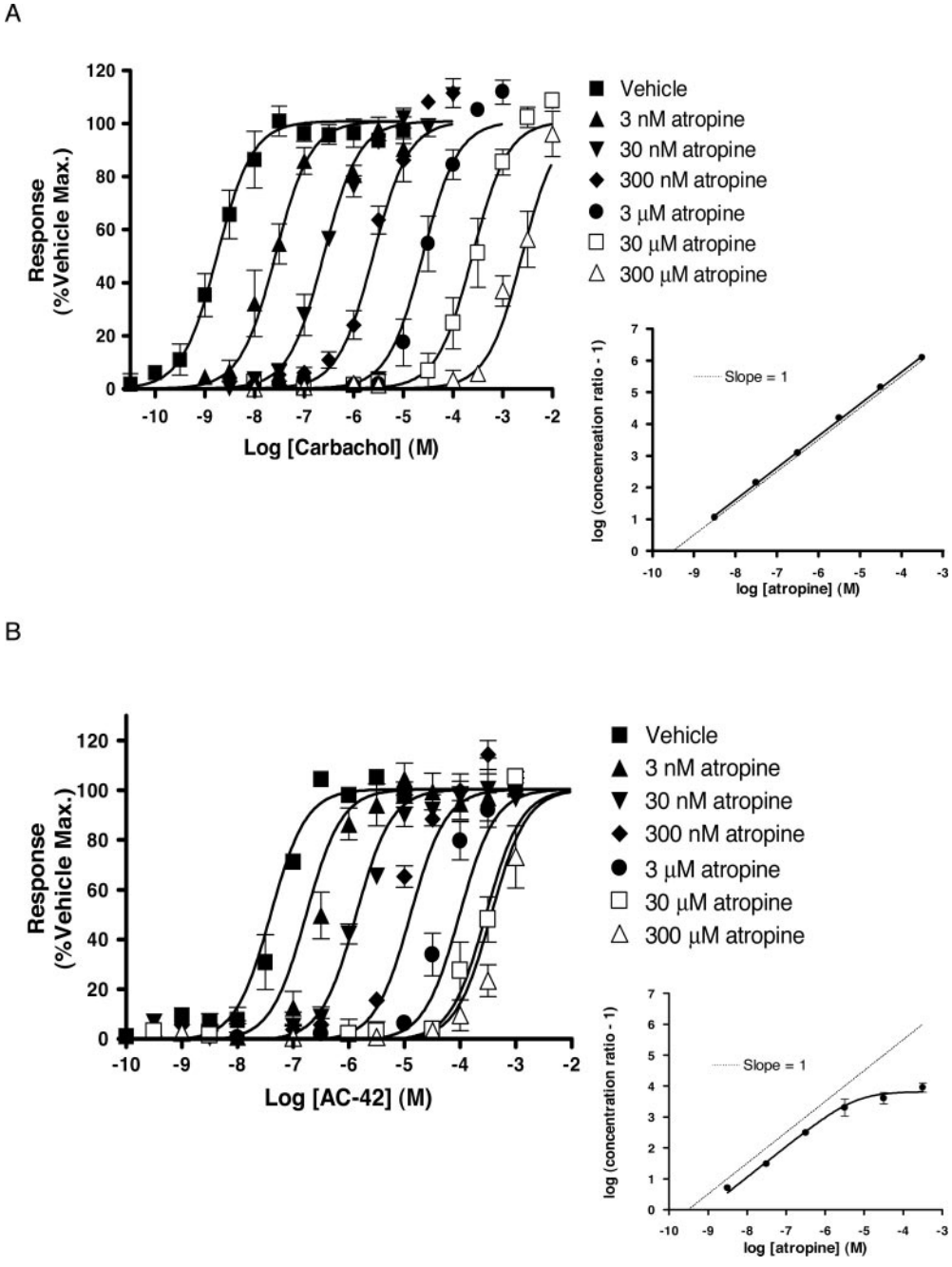

Fig. 5. Concentration-dependent antagonism of carbachol-stimulated (A) or AC-42-stimulated (B) calcium mobilization in CHO-hM_1 cells by atropine (3 nM–300 nM) with inset Schild regressions. Dotted lines on Schild plots indicate a theoretical slope of 1. Data are the mean of at least three independent experiments (±S.E.M.).

exhibited by atropine when tested against AC-42. However, the conclusion from our experiments is that AC-42 must be the allosteric ligand, because atropine is a well characterized orthosteric antagonist of mAChRs. Subsequent analysis of the data according to an allosteric ternary complex model yielded a pK_B estimate for atropine (Table 2) that was in good agreement with its known affinity for the orthosteric site but that also provided an estimate of the cooperativity between atropine and AC-42 ($\alpha = 0.0002$). Thus, it can be concluded that the low Schild slopes associated with the interaction between atropine or pirenzepine and AC-42 actually reflect the saturability (governed by α in the ternary complex model) of an allosteric interaction between antagonist and agonist. Unfortunately, we could not estimate α values for the interaction between pirenzepine and AC-42 because of the limited number of antagonist concentrations that were able to be studied.

More direct evidence of an allosteric mode of action for AC-42 was obtained using radioligand binding. It is well established that allosteric modulators can have characteristic effects on the binding of orthosteric ligands (Christopoulos and Kenakin, 2002). For example, binding studies using two or more radioligand concentrations can reveal differences in the binding isotherm of the allosteric modulator because the saturability in the allosteric event becomes more evident as the concentration of orthosteric radioligand is increased (Christopoulos and Kenakin, 2002). Therefore, and in contrast to atropine and pirenzepine (Fig. 6A), AC-42 was unable to fully inhibit the specific binding of [^{3}H]NMS at either 0.2 nM, or more strikingly, at the higher radioligand concentration of 2 nM, a property that was shared by the prototypical modulator gallamine (Fig. 6B). The values derived for gallamine via the application of an allosteric model are in good agreement with similar values determined previously (Matsui et al., 1995), whereas our study is the first to apply such a model to AC-42. It is noteworthy that the estimated α value for the interaction between AC-42 and [^{3}H]NMS was significantly different from the value describing the interaction between AC-42 and atropine. This highlights a second characteristic of allosteric interactions (in addition to saturability), namely, that the degree of cooperativity between orthosteric and allosteric sites depends on the chemical nature of the ligands occupying each site. This probe dependence of allosterism can explain why in some studies, an allosteric interaction may be missed altogether if it is characterized by either neutral cooperativity (i.e., seems as if there is no interaction) or by very high negative cooperativity (i.e., seems as if the interaction is competitive).

A further method used to validate an allosteric mechanism of action is to monitor the effects of a putative modulator on the dissociation of a preformed orthosteric ligand-receptor complex. Any alteration in the dissociation of such a complex

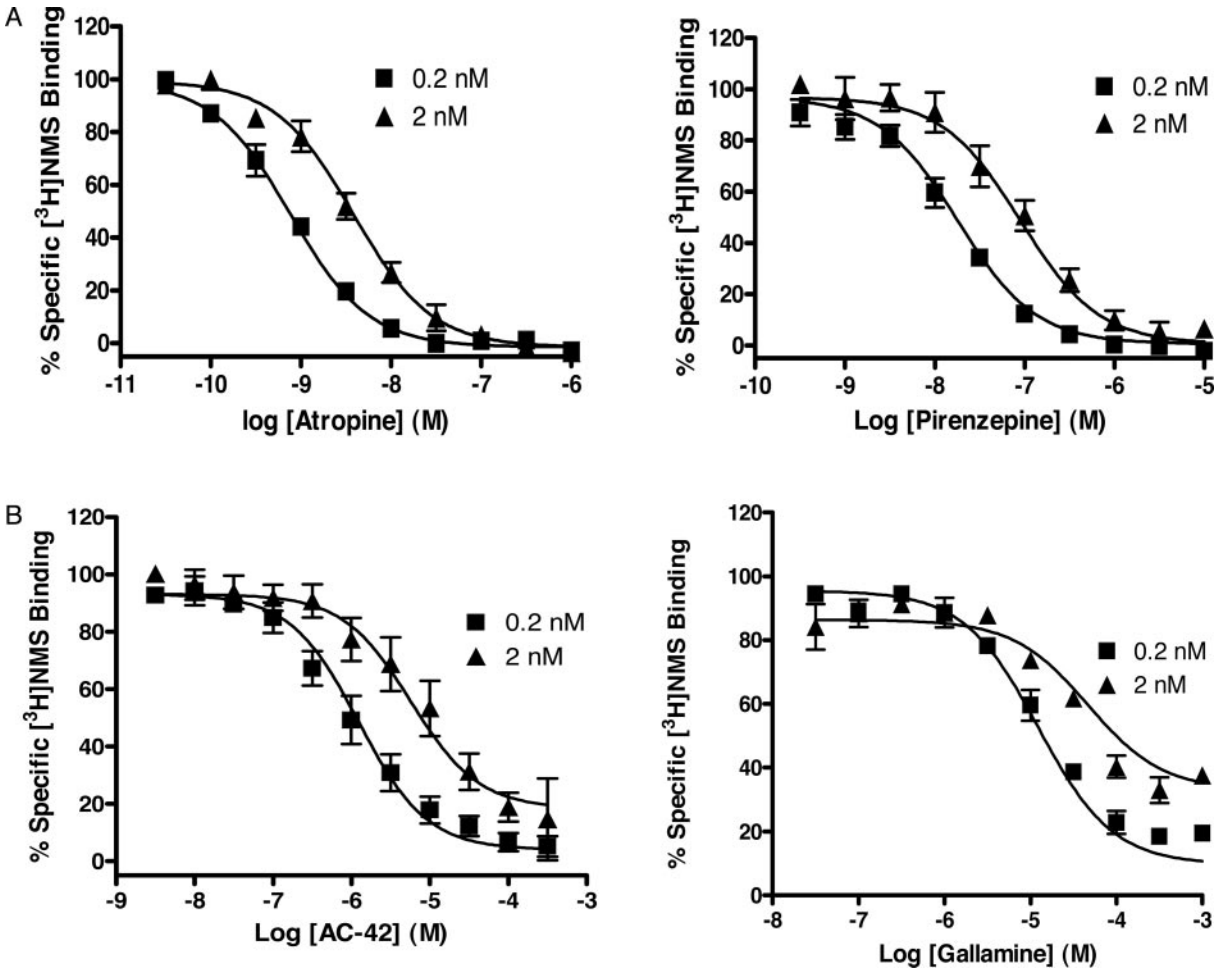

Fig. 6. Inhibition of 0.2 and 2 nM [^{3}H]NMS binding in CHO-hM$_1$ cell membranes by atropine or pirenzepine (A) or AC-42 or gallamine (B). Data are the mean of at least three independent experiments (±S.E.M.).

must be indicative of a conformational change mediated via a topographically distinct site (Kostenis and Mohr, 1996). Indeed, prototypical allosteric modulators of mAChRs, such as C_7/3-phth (Christopoulos et al., 1999), strychnine (Lazareno and Birdsall, 1995), and gallamine (Stockton et al., 1983) have all been shown to allosterically retard the rate of [^{3}H]NMS dissociation from mAChRs in a concentration-dependent manner. Thus, the most striking confirmation of the allosteric nature of AC-42 and gallamine was obtained from [^{3}H]NMS dissociation kinetic assays. As illustrated in Fig. 7, both AC-42 and gallamine retarded the dissociation of [^{3}H]NMS from the M_1 mAChR. This effect was much more pronounced for gallamine for at least two reasons. First, at the concentrations of each modulator used in the kinetic assays (reflecting solubility maxima), it can be calculated from their relative K_B and α values that 1 mM gallamine would occupy ca. 98% of the [^{3}H]NMS-bound receptors, whereas 100 μM AC-42 would only occupy ca. 77% of the [^{3}H]NMS-bound receptors. Second, it is possible that AC-42 simply cannot exert the same maximal effect on radioligand kinetics as gallamine.

As a whole, the data presented here provide unambiguous evidence that AC-42 is appropriately classed as an allosteric, rather than an ectopic, agonist of the muscarinic M_1 receptor; i.e., it meets all the criteria for classification as an allosteric ligand in addition to possessing efficacy at the receptor in the absence of other ligands. The prevalence of other confirmed allosteric agonists of G protein-coupled receptors remains relatively limited in the current literature. There is some evidence that the adenosine A_1 receptor enhancer PD 81,723 is able to promote a modest degree of receptor G protein-coupling in its own right (Bhattacharya and Linden, 1995). Likewise, the peptide ASLW has been shown to activate the chemokine CXCR4 receptor in a manner that is likely to be allosteric (Sachpatzidis et al., 2003). For the mAChRs, Jakubik et al. (1996) demonstrated that gallamine and alcuronium could promote receptor activation, but these results are not consistently reproduced (Lazareno and Birdsall, 1995; May et al., 2005) and may reflect the requirement of particular stoichiometries of receptor to G protein (Jakubik et al., 1998). Earlier radioligand binding studies suggested that the partial agonist McN-A-343 was also an allosteric modulator of M_2 mAChRs (Birdsall et al., 1983), although a subsequent functional study was unable to conclude whether this compound interacted allosterically with very high negative cooperativity or via simple orthosteric competition when tested against carbachol (Christopoulos and Mitchelson, 1997).

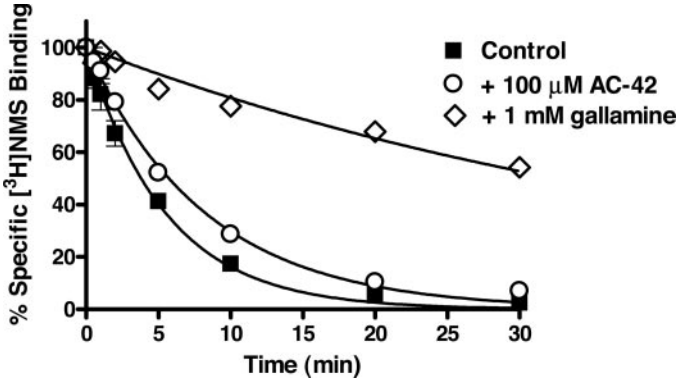

Fig. 7. Effect of AC-42 (100 μM) or gallamine (1 mM) on atropine (1 μM)-induced dissociation of [^{3}H]NMS from CHO-hM_1 cell membranes. Data are the mean of at least three independent experiments (±S.E.M.).

In contrast, we have now shown, using functional, equilibrium binding, and dissociation kinetic assays that the mechanism of action of AC-42 at the M_1 mAChR is qualitatively and quantitatively consistent with an allosteric model. This finding not only has important ramifications for mAChR-based drug discovery but also raises additional considerations. For example, is the allosteric site recognized by AC-42 the same site as that recognized by gallamine, a second allosteric site recognized by certain staurosporine derivatives (Lazareno et al., 2000), or a third topographically distinct allosteric site? What is it about the nature of the AC-42 binding site that allows almost exclusive activation of the M_1 mAChR relative to other mAChR subtypes? Further studies are clearly warranted to elucidate the molecular nature of this allosteric site.

References

Arunlakshana O and Schild HO (1959) Some quantitative uses of drug antagonists. *Br J Pharmacol* **14:**48–57.

Bhattacharya S and Linden J (1995) The allosteric enhancer, PD 81,723, stabilizes human A_1 adenosine receptor coupling to G proteins. *Biochim Biophys Acta* **1265:** 15–21.

Birdsall NJM, Burgen ASV, Hulme EC, Stockton JM, and Zigmond MJ (1983) The effect of McN-A-343 on muscarinic receptors in the cerebral cortex and heart. *Br J Pharmacol* **78:**257–259.

Bradford MM (1976) A rapid and sensitive method for the quantitation of microgram quantities of protein utilizing the principle of protein-dye binding. *Anal Biochem* **72:**248–254.

Brandish PE, Hill LA, Zheng W, and Scolnick EM (2003) Scintillation proximity assay of inositol phosphates in cell extracts: high-throughput measurement of G-protein-coupled receptor activation. *Anal Biochem* **313:**311–318.

Caulfield MP and Birdsall NJ (1998) International Union of Pharmacology. XVII. Classification of muscarinic acetylcholine receptors. *Pharmacol Rev* **50:**279–290.

Christopoulos A (1998) Assessing the distribution of parameters in models of ligand-receptor interaction: to log or not to log. *Trends Pharmacol Sci* **19:**351–357.

Christopoulos A and Kenakin T (2002) G protein-coupled receptor allosterism and complexing. *Pharmacol Rev* **54:**323–374.

Christopoulos A and Mitchelson F (1997) Pharmacological analysis of the mode of interaction of McN-A-343 at atrial muscarinic M_2 receptors. *Eur J Pharmacol* **339:**153–156.

Christopoulos A, Sorman JL, Mitchelson F, and El-Fakahany EE (1999) Characterization of the subtype selectivity of the allosteric modulator heptane-1,7-bis-(dimethyl-3′-phthalimidopropyl)ammonium bromide (C7/3-phth) at cloned muscarinic acetycholine receptors. *Biochem Pharmacol* **57:**171–179.

Clark AL and Mitchelson F (1976) The inhibitory effects of gallamine on muscarinic receptors. *Br J Pharmacol* **58:**323–331.

Ehlert FJ (1988) Estimation of the affinities of allosteric ligands using radioligand binding and pharmacological null methods. *Mol Pharmacol* **33:**187–194.

Ellis J (2002) Muscarinic receptors, in *Understanding G Protein-Coupled Receptors and Their Role in the CNS* (Pangalos MN and Davies CH eds) pp 349–371, Oxford University Press, Oxford, UK.

Gnagey AL, Seidenberg M, and Ellis J (1999) Site-directed mutagenesis reveals two epitopes involved in the subtype selectivity of the allosteric interactions of gallamine at muscarinic acetylcholine receptors. *Mol Pharmacol* **56:**1245–1253.

Jakubik J, Bacakova L, Lisa V, el-Fakahany EE, and Tuček S (1996) Activation of muscarinic acetylcholine receptors via their allosteric binding sites. *Proc Natl Acad Sci USA* **93:**8705–8709.

Jakubík J, Haga T, and Tuček S (1998) Effects of an agonist, allosteric modulator and antagonist on guanosine-γ-[^{35}S]thiotriphosphate binding to liposomes with varying muscarinic receptor/G_o protein stoichiometry. *Mol Pharmacol* **54:**899–906.

Kenakin TP (1997) *Pharmacologic Analysis of Drug-Receptor Interaction*, Lippincott-Raven Publishers, Philadelphia, PA.

Kostenis E and Mohr K (1996) Two-point kinetic experiments to quantify allosteric effects on radioligand dissociation. *Trends Pharmacol Sci* **17:**280–283.

Kristiansen K (2004) Molecular mechanisms of ligand binding, signaling and regulation within the superfamily of G-protein-coupled receptors: molecular modeling and mutagenesis approaches to receptor structure and function. *Pharmacol Ther* **103:**21–80.

Lanzafame A and Christopoulos A (2004) Investigation of the interaction of a putative allosteric modulator, *N*-(2,3-diphenyl-1,2,4-thiadiazole-5-(2*H*)-ylidene) methanamine hydrobromide (SCH-202676), with M_1 muscarinic acetylcholine receptors. *J Pharmacol Exp Ther* **308:**830–837.

Lanzafame A, Christopoulos A, and Mitchelson F (1996) Interactions of agonists with an allosteric antagonist at muscarinic acetylcholine M_2 receptors. *Eur J Pharmacol* **316:**27–32.

Lazareno S and Birdsall NJ (1995) Detection, quantitation and verification of allosteric interactions of agents with labeled and unlabeled ligands at G protein-coupled receptors: interactions of strychnine and acetylcholine at muscarinic receptors. *Mol Pharmacol* **48:**362–378.

Lazareno S, Popham A, and Birdsall NJ (2000) Allosteric interactions of staurospor-

ine and other indolocarbazoles with *N*-[methyl-^{3}H]scopolamine and acetylcholine at muscarinic receptor subtypes: identification of a second allosteric site. *Mol Pharmacol* **58:**194–207.

Matsui H, Lazareno S, and Birdsall NJ (1995) Probing of the location of the allosteric site on m1 muscarinic receptors by site-directed mutagenesis. *Mol Pharmacol* **47:**88–98.

May LT, Lin Y, Sexton PM, and Christopoulos A (2005) Regulation of M2 muscarinic acetylcholine receptor expression and signaling by prolonged exposure to allosteric modulators. *J Pharmacol Exp Ther* **312:**382–390.

Motulsky HJ and Christopoulos A (2004) *Fitting Models to Biological Data Using Linear and Nonlinear Regression. A Practical Guide to Curve Fitting*, Oxford University Press, New York.

Spalding TA, Trotter C, Skjaerbaek N, Messier TL, Currier EA, Burstein ES, Li D, Hacksell U, and Brann MR (2002) Discovery of an ectopic activation site on the M_1 muscarinic receptor. *Mol Pharmacol* **61:**1297–1302.

Sachpatzidis A, Benton BK, Manfredi JP, Wang H, Hamilton A, Dohlman HG, and Lolis E (2003) Identification of allosteric peptide agonists of CXCR4. *J Biol Chem* **278:**896–907.

Stockton JM, Birdsall NJ, Burgen AS, and Hulme EC (1983) Modification of the binding properties of muscarinic receptors by gallamine. *Mol Pharmacol* **23:** 551–557.

Sur C, Mallorga PJ, Wittmann M, Jacobson MA, Pascarella D, Williams JB, Brandish PE, Pettibone DJ, Scolnick EM, and Conn PJ (2003) N-Desmethylclozapine, an allosteric agonist at muscarinic 1 receptor, potentiates N-methyl-D-aspartate receptor activity. *Proc Natl Acad Sci USA* **100:**13674–13679.

Ward SD, Curtis CA, and Hulme EC (1999) Alanine-scanning mutagenesis of transmembrane domain 6 of the M_1 muscarinic acetylcholine receptor suggests that Tyr381 plays key roles in receptor function. *Mol Pharmacol* **56:**1031–1041.

Address correspondence to: Dr. Christopher J. Langmead, Psychiatry CEDD, GlaxoSmithKline, Third Ave., Harlow, Essex, CM19 5AW, UK. E-mail: christopher.j.langmead@gsk.com